THE JOURNAL OF BIOLOGICAL CHEMISTRY VOL. 284, NO. 36, pp. 24453–24464, September 4, 2009

Inhibition of Lysine Acetyltransferase KAT3B/p300 Activity by a Naturally Occurring Hydroxynaphthoquinone, Plumbagin*[S]

Received for publication, May 22, 2009, and in revised form, June 29, 2009 Published, JBC Papers in Press, July 1, 2009, DOI 10.1074/jbc.M109.023861

Kodihalli C. Ravindra[‡1], B. Ruthrotha Selvi[‡1,2], Mohammed Arif[‡2], B. A. Ashok Reddy[‡], Gali R. Thanuja[‡], Shipra Agrawal[§], Suman Kalyan Pradhan[¶], Natesh Nagashayana[‖], Dipak Dasgupta[¶], and Tapas K. Kundu[‡3]

From the [‡]Transcription and Disease Laboratory, Molecular Biology and Genetics Unit, Jawaharlal Nehru Centre for Advanced Scientific Research, Jakkur, Bangalore 560064, [§]Institute of Bioinformatics and Applied Biotechnology, International Technology Park Bangalore, Whitefield Road, Bangalore 560066, [‖]Central Government Health Scheme Dispensary Number 3, Basavanagudi, Bangalore 560004, and [¶]Biophysics Division, Saha Institute of Nuclear Physics, I/AF, Bidhan Nagar, Kolkata 700064, India

Lysine acetyltransferases (KATs), p300 (KAT3B), and its close homologue CREB-binding protein (KAT3A) are probably the most widely studied KATs with well documented roles in various cellular processes. Hence, the dysfunction of p300 may result in the dysregulation of gene expression leading to the manifestation of many disorders. The acetyltransferase activity of p300/CREB-binding protein is therefore considered as a target for new generation therapeutics. We describe here a natural compound, plumbagin (RTK1), isolated from *Plumbago rosea* root extract, that inhibits histone acetyltransferase activity potently *in vivo*. Interestingly, RTK1 specifically inhibits the p300-mediated acetylation of p53 but not the acetylation by another acetyltransferase, p300/CREB-binding protein -associated factor, PCAF, *in vivo*. RTK1 inhibits p300 histone acetyltransferase activity in a noncompetitive manner. Docking studies and site-directed mutagenesis of the p300 histone acetyltransferase domain suggest that a single hydroxyl group of RTK1 makes a hydrogen bond with the lysine 1358 residue of this domain. In agreement with this, we found that indeed the hydroxyl group-substituted plumbagin derivatives lost the acetyltransferase inhibitory activity. This study describes for the first time the chemical entity (hydroxyl group) required for the inhibition of acetyltransferase activity.

The eukaryotic genome is organized in a highly complex nucleoprotein structure, chromatin. Physiologically, chromatin is not just a DNA and histone complex, rather it is a dynamic organization of DNA associated with histone, histone-interacting non-histone proteins, and RNA (1). The hallmark of chromatin is its dynamic nature, which is essential for the regulation of nuclear processes that require access to genetic information. This dynamicity of chromatin is maintained by several factors, including the post-translational modifications of histone and non-histone chromatin components, especially the reversible acetylation (2). The enzymatic activity of the acetyltransferases and deacetylases sets up a fine balance that maintains the cellular homeostasis (3). Any imbalance in this may result in disease manifestation.

Chromatin acetylation is catalyzed by five different classes of lysine acetyltransferases (4). Among these, the best studied is p300 and its close homologue CBP.[4] p300 has been shown to regulate various biological phenomena such as proliferation, cell cycle regulation, apoptosis, differentiation, and DNA damage response (5–8). It is a potent transcriptional coactivator. Therefore, dysfunction of p300 may have deleterious effects on various cellular functions and thus could be the underlying cause of several diseases, especially cancer. Acetyltransferase activity has been considered as a target for new generation therapeutics (3, 9). The therapeutic potential of HAT inhibitors has been shown in cancer (10–12), cardiac diseases (13), diabetes mellitus (14), and human immunodeficiency virus (15).

Unlike the histone deacetylase inhibitors, the acetyltransferase inhibitors are relatively fewer in number. Recently, however, a few potent as well as specific KAT inhibitors have been discovered (Table 1). Among these, curcumin was found to be the only known p300-specific natural inhibitor, which is also cell-permeable (16). Therefore, there is an active ongoing effort to identify modulators (activator/inhibitor) targeted toward p300 activity. Here we report that plumbagin, a hydroxynaphthoquinone (Fig. 1*A*) isolated from the roots of *Plumbago rosea* (known in Indian ayurvedic medicine as Chitraka), is a potent acetyltransferase inhibitor *in vivo*. Most of the known KAT inhibitors, possess polyhydroxy functional groups, whereas plumbagin has a single hydroxyl group. The substitution of this group with other moieties resulted in a complete loss of the p300 inhibitory activity. Therefore, these data for the first time establish the chemical entity (functional group) responsible for p300 inhibition.

MATERIALS AND METHODS

Isolation and Purification of Plumbagin from P. rosea Roots

The dried and powdered roots of *P. rosea* (100 g) were extracted with ethyl acetate. The ethyl acetate extract after

* This work was supported by the Department of Biotechnology, Government of India, and Jawaharlal Nehru Centre for Advanced Scientific Research.

[S] The on-line version of this article (available at http://www.jbc.org) contains supplemental Figs. 1–6 and additional text for spectral details of different RTK1 derivatives.

[1] Both authors contributed equally to this work.

[2] Senior Research Fellow of the Council of Scientific and Industrial Research.

[3] To whom correspondence should be addressed: Transcription and Disease Laboratory, Molecular Biology and Genetics Unit, Jawaharlal Nehru Centre for Advanced Scientific Research, Jakkur, Bangalore 560064, India. Tel.: 91-80-2208-2840; Fax: 91-80-2208-2766; E-mail: tapas@jncasr.ac.in.

[4] The abbreviations used are: CBP, CREB-binding protein; HAT, histone acetyltransferase; CC, column chromatography; KAT, lysine acetyltransferase; PCAF, p300/CBP-associated factor; ITC, isothermal titration calorimetry.

TABLE 1
HAT inhibitors

Serial No.	HAT inhibitor	Target	Ref.
1	Lysyl-CoA	p300	34
2	H3-CoA-20	PCAF	34
3	Anacardic acid	p300/PCAF/CBP	30
4	Garcinol	p300/PCAF/CBP	16
5	Curcumin	p300/CBP	16
6	γ-Butyrolactones	CBP/Gcn5	35
7	Isothiazolones	p300/PCAF	11
8	LTK14	p300	17
9	Epigallocatechin 3-gallate	HATs	29

removal of the solvent under reduced pressure gave a dark brown semisolid, which was separated into phenolic and neutral fractions by treatment with 5% NaOH and followed by acidification with 2 M HCl and extraction with diethyl ether. The phenolic fraction was subjected to flash chromatography (230–400 mesh) using increasing polarity. The fraction extracted with 4% ethyl acetate in hexane mixture gave an orange solid, which on further recrystallization yielded plumbagin/RTK1 (0.286 g). The yielded compound was compared with commercially available material.

Immunoblotting Analysis

HepG2 cells (1.5×10^6 cells per 60-mm dish) were seeded overnight, and histones were extracted by acid extraction after 12 h of treatment with increasing concentrations of plumbagin. Immunoblotting analysis was performed as described elsewhere (17), using polyclonal acetylated histone H3 and polyclonal histone H3 antibodies.

Immunofluorescence Analysis

To visualize the inhibition of histone acetylation *in vivo*, HeLa cells were cultured as a monolayer on the poly-L-lysine-coated coverslips in Dulbecco's modified Eagle's medium (Sigma). Immunofluorescence was carried out as described elsewhere (17). Fixed cells were probed with anti-acetylated histone H3 polyclonal antibodies followed by secondary antibody conjugated with Alexa 488 (Invitrogen). To stain the chromosomal DNA, Hoechst 33528 (Sigma) was used. The images were taken by using Zeiss LSM 510 laser scanning confocal microscope.

Immunohistochemical Analysis of Mice Liver on Plumbagin Treatment

Plumbagin (25 mg/kg body weight) dissolved in 50 μl of DMSO was injected intraperitoneally to 2-month-old Swiss albino mice. As controls, two mice were injected with 50 μl of water and 50 μl of DMSO intraperitoneally as negative control and solvent control, respectively. The experiment was done in triplicate. All mice were staged in animal cages for the next 6 h and anesthetized, and the liver was collected for further protein, RNA, and immunohistochemical analysis.

Liver samples stored in formalin were further dehydrated in alcohol, followed by xylene treatment, and allowed to get impregnated in paraffin blocks. 3–4-μm thick paraffin-embedded sections were deparaffinized in xylene, followed by rehydration in decreasing concentrations of ethanol solutions. For routine pathological examination, deparaffinized sections from all blocks were stained with hematoxylin and eosin stains. Antigen retrieval was performed by microwaving in appropriate buffer. After washing the sections in 0.1 M phosphate buffer, blocking was done using 3% skimmed milk, following which the sections were incubated with anti-AcH3 antibody for 3 h in a humidification chamber. After 0.1 M phosphate buffer wash, the sections were incubated with link secondary antibody (DAKO LSAB$^+$) for 3 h in a humidification chamber. After washing, the sections were developed with 3′,3′-diaminobenzidine tetrahydrochloride (Sigma). Hematoxylin was used as counterstain to identify the unstained nucleus.

p53 Modulation Assays

HEK293 cells were incubated for 3 h with 2.5, 5, and 10 μM plumbagin. After the compound treatment, the cells were treated with 500 ng/ml doxorubicin for 6 h. The cells were then harvested and lysed in TNN buffer (150 mM NaCl, 50 mM Tris, pH 7.4, 1% Nonidet P-40, 0.1% sodium deoxycholate, 1 mM EDTA, 0.5 μg/ml leupeptin, 0.5 μg/ml aprotinin, and 0.5 μg/ml pepstatin) for 3 h on ice with intermittent mixing. The whole cell lysates from the treated cells were subjected to Western blotting analysis by using mouse monoclonal anti-p53 antibody, DO1 (Calbiochem), rabbit polyclonal acetylated p53 Lys-373, and Lys-320 antibodies (Upstate) and tubulin antibody (Calbiochem).

Histone Acetyltransferase Assay

HAT assays were performed as described previously (17). 2.4 μg of highly purified HeLa core histones were incubated in HAT assay buffer at 30 °C for 10 min with or without baculovirus-expressed recombinant p300 or PCAF in the presence and absence of compounds followed by addition of 1.0 μl of 3.6 Ci/mmol of [^{3}H]acetyl-CoA (PerkinElmer Life Sciences) and further incubated for another 10 min in a 30-μl reaction. The reaction mixture was then blotted onto P81 (Whatman) filter paper, and radioactive counts were recorded on a Wallac 1409 liquid scintillation counter.

Protein Methyltransferase Assay

2.4 μg of highly purified HeLa core histones along with CARM1 (20 ng)/G9a (15 ng) were incubated in the buffer containing 20 mM Tris, pH 8.0, 4 mM EDTA, pH 8.0, 200 mM NaCl, and 1 μl of 15 Ci/mmol of *S*-[^{3}H]adenosylmethionine (Amersham Biosciences), either in the presence or absence of compound in a final reaction volume of 30 μl at 30 °C for 30 min. The reaction was stopped on ice for 5 min before blotting onto P81 (Whatman) filter paper. The radioactive counts were recorded on Wallac 1409 Liquid Scintillation counter.

p300 HAT Domain Purification

The recombinant minimal HAT domain was purified as described elsewhere (18).

Kinetic Characterization of RTK1-mediated p300 Inhibition

The HAT reactions were carried out with the baculovirus-expressed recombinant full-length p300, in the presence of different concentrations of the inhibitor RTK1 (15, 20, 35, and 45 μM). The HAT reaction consists of two substrates, core his-

tones and the acetyl group donor [^{3}H]acetyl-CoA. Therefore, the kinetic analysis was done in two different sets. In the first set, concentration of core histones was kept constant at 1.6 μM, and [^{3}H]acetyl-CoA was varied from 1.08 to 8.66 μM. In the second assay, [^{3}H]acetyl-CoA was kept constant at 2.78 μM, and core histones were varied from 0.003 to 0.068 μM. The incorporation of the radioactivity was taken as a measure of the reaction velocity recorded as counts/min. Each experiment was performed in triplicate, and the reproducibility was found to be within 15% of the error range. Weighted averages of the values obtained were plotted as a Lineweaver-Burk plot using GraphPad Prism software.

Isothermal Titration Calorimetry (ITC)

ITC experiments were carried out in a VP-ITC system (Microcal LLC) at 25 °C. Samples were centrifuged and degassed prior to titration. Titration of RTK1/RTK2 against the protein HAT domain was carried out by injecting 0.2 mM RTK1/RTK2 in 20 mM Tris, pH 7.5, 0.2 mM EDTA, 100 mM KCl buffer against 0.0034 mM HAT domain. A 2-min interval was allowed between injections for equilibration. A total of 40 injections was carried out to ensure complete titration. The protein concentration was chosen to achieve sufficiently high heat signals with a minimum enthalpy of dilution. To minimize the error associated with diffusion from the syringe during base-line equilibration, the first injection was only 1 μl, and the associated small heat change was not considered for data analysis. Blank titrations were carried out using buffer and DMSO with no ligand against the HAT domain and used for subtraction of the background heat change. The corrected heat changes were plotted against the molar ratio of the titrated products and analyzed using the manufacturer's software, which yielded the stoichiometry n (in terms of number of molecules of RTK1/protein), equilibrium constant (K_a). From the relationship $\Delta G^0 = -RT \ln K_a$ and the Gibbs-Helmholtz equation, the free energy of binding and the entropy of association (ΔS^0) were calculated.

Docking Studies

Crystal structure of p300 HAT domain was extracted from Protein Data Bank code 3BIY. Crystal structure of the inhibitor RTK1 and its inactive derivative RTK2 was obtained and solved (Bruker X8 APEX). The HAT domain was docked with the structure of RTK1 and RTK2 to find out their interaction sites on HAT domain. RTK1 has a hydroxyl group at the 5th carbon position, and the derivative RTK2 has a methoxy group instead of the hydroxyl group.

Molecular simulation and the docking of HAT domain with RTK1 and RTK2 were performed using Hex 4.5 software. The docking calculations were done using three-dimensional parametric functions of both the protein (HAT domain) and the chemical structures (RTK1/RTK2). These calculations were used to encode surface shape and electrostatic charge and potential distributions. The parametric functions are based on expansions of real orthogonal spherical polar basis functions. The docking was performed in full rotation mode; both domain and inhibitor were taken at 180 ranges for 20,000 solutions.

Site-directed Mutagenesis

Site-directed mutagenesis was done to obtain a HAT domain point mutant K1358A. HAT domain expression clone in pET28b was used as the template, and the mutagenesis was done by the Stratagene site-directed mutagenesis kit according to the manufacturer's instructions. The positive clones were sequenced and transformed into BL21 strain of *Escherichia coli*. The expression and purification of the mutant protein was done as mentioned elsewhere (18).

General Methods

NMR spectroscopy, TLC, and x-ray characterization of the compounds were done as described elsewhere (17). High resolution mass spectrometry was obtained on a Bruker Daltonics APEX II (for electrospray ionization).

Synthesis of Plumbagin/RTK1 Derivatives

RTK2, 5-Methoxy-2-methyl-1,4-naphthoquinone—The solution of RTK1 (100 mg, 0.53 mmol) in acetone, anhydrous potassium carbonate (146 mg, 1 mmol) was stirred for about 10 min, and then methyl iodide (43 mg, 0.3 mmol) was added dropwise and the stirring continued for about 2 h. The reaction was monitored by TLC. Then solvent was evaporated to dryness and subjected to column chromatography, which yielded the compound RTK2.

RTK3, 5-Ethoxy-2-methyl-1,4-naphthoquinone—Ethyl iodide (55 mg, 0.35 mmol) was added dropwise to the solution mixture of RTK1 (100 mg, 0.53 mmol) and anhydrous potassium carbonate (146 mg, 1 mmol) in acetone for about 20 min, and the reaction mixture was stirred for 2 h. The solvent was evaporated to dryness and subjected to CC to yield RTK3.

RTK4, 5-Isopropoxy-2-methyl-1,4-naphthoquinone—The mixture of RTK1 (100 mg, 0.53 mmol) and anhydrous potassium carbonate (146 mg, 1 mmol) in acetone was stirred for about 10 min in a two-necked round bottom flask. Isopropyl iodide (63 mg, 0.37 mmol) was then added dropwise, and stirring was continued for another 2 h. The solvent was evaporated under reduced pressure and subjected to CC to yield compound RTK4.

RTK5, 6-Methyl-5,8-dioxo-5,8-dihydronaphthalen-1-yl Acetate—A solution of RTK1 (100 mg, 0.53 mmol) in dichloromethane was added to a cooled solution of triethylamine (148 mg, 1.4 mmol) in dichloromethane. The reaction mixture was stirred for 30 min at 0–5 °C, and then acetyl chloride (56 mg, 0.71 mmol) was slowly added into the reaction mixture for a period of 30 min. After stirring at 0–5 °C for 6 h, the temperature was slowly increased to 20–25 °C and again stirred for 4 h. The solvent was evaporated to dryness and purified by CC resulting in compound RTK5.

RTK6, 6-Methyl-5,8-dioxo-5,8-dihydronaphthalen-1-yl Methanesulfonate—RTK1 (100 mg, 0.53 mmol) was dissolved in dichloromethane (10 ml). Triethylamine (148 mg, 1.4 mmol) was added, and the reaction mixture was cooled to 0–5 °C. Methylsulfonyl chloride was slowly added (61 mg, 0.538 mmol) in dichloromethane. The reaction mixture was stirred for 4 h at 0–5 °C, and the temperature was raised slowly to 20–25 °C and stirred for 8–10 h. The resulting reaction mixture was isolated and subjected to CC to yield RTK6.

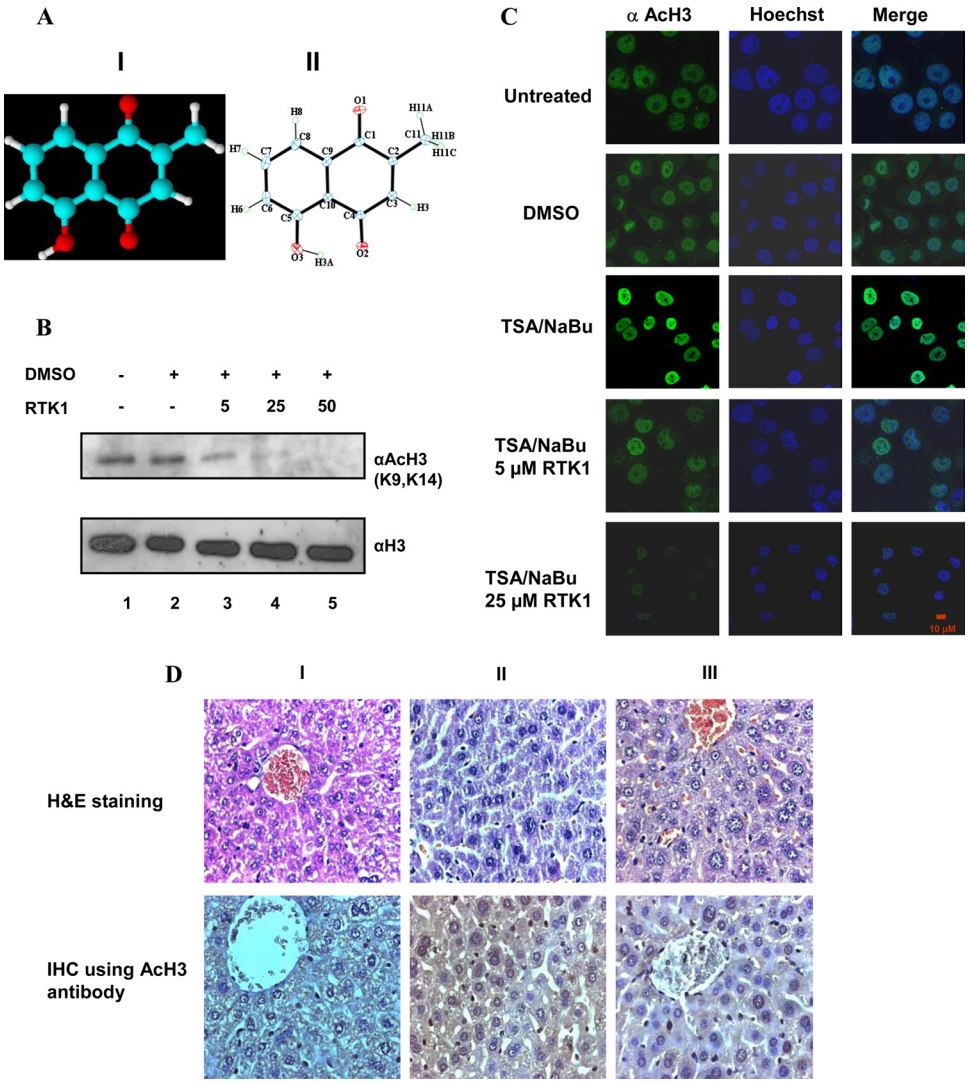

FIGURE 1. **RTK1 is a potent inhibitor of histone acetylation *in vivo*.** *A, panel I, ball* and *stick model* of RTK1, where *blue* denotes carbon; *white* indicates hydrogen; and *red* represents oxygen; *panel II,* x-ray crystal structure of RTK1 is shown. *B,* HepG2 cells were treated as indicated for 12 h; histones were isolated from untreated cells (*lane 1*). DMSO-treated cells (*lane 2*), RTK1-treated cells (*lanes 3–5*). The histone acetylation was probed by immunoblotting using acetylated H3 antibody. As a loading control the blots were probed with histone H3 antibody. *C,* inhibition of histone acetylation was visualized by immunofluorescence analysis of RTK1-treated HeLa cells probed with antibodies against acetylated histone H3. The Hoechst-stained images represent DNA. Cells were either treated with DMSO or with RTK1 (10 μM and 25 μM) in the presence of trichostatin A and sodium butyrate (*TSA/NaBu*) as indicated for 12 h. *D,* liver tissue from mice injected with water (*panel I*), DMSO (*panel II*), and RTK1 (*panel III*) was stained with hematoxylin and eosin (*H&E*) or immunostained with antiacetylated histone H3 antibody as indicated.

RTK7, 2-Methyl-5-(2-piperidin-1-ylethoxy)-1,4-naphthoquinone—RTK1 solution (100 mg, 0.53 mmol) in ethanol (20 ml), potassium hydroxide (59 mg, 1 mmol) was taken in a round bottom flask and stirred for about 10 min, followed by addition of 1-(2-chloroethyl)piperidine hydrochloride (117 mg, 0.63 mmol), and the reaction mixture was heated to 60 °C. After 2 h, the reaction mixture was cooled to room temperature, poured into water, acidified with dilute HCl, and extracted with ethyl acetate. The extract was evaporated to get residue, which was subjected to CC to get RTK7.

RTK8, 2-Methyl-5-(2-morpholin-4-ylethoxy)-1,4-naphthoquinone—The 4-(2-chloroethyl)morpholine hydrochloride (118 mg, 0.63 mmol) was added into the reaction mixture of RTK1 (100 mg, 0.53 mmol) and potassium hydroxide (59 mg, 1 mmol) in ethanol. The reaction mixture was heated up to 60 °C over a period of 90 min followed by cooling. The mixture was poured into ice-cold water and acidified with dilute HCl to pH 7.0 and extracted with ethyl acetate. The extract was evaporated to get residue and subjected to CC to yield RTK8.

RTK9, Ethyl [(6-Methyl-5,8-dioxo-5,8-dihydronaphthalen-1-yl)-oxy]acetate—The solution of RTK1 in acetone (100 mg, 0.53 mmol) and potassium carbonate (146 mg, 1 mmol) was stirred at room temperature for about 10 min followed by addition of ethyl bromoacetate (76 mg, 0.46 mmol), and the temperature was slowly increased to 50 °C. The reaction mixture was heated for about 2 h and poured into ice and acidified with dilute HCl (to pH 7) and then extracted with ethyl acetate. The extract was evaporated to get residue, which was subjected to CC to get RTK9.

RTK10, 5-[2-(Dimethylamino)-ethoxy]-2-methyl-1,4-naphthoquinone—RTK1 solution (100 mg, 0.53 mmol) in ethanol, potassium hydroxide (59 mg, 1 mmol) were taken in a two-necked round bottom flask, stirred for about 10 min, followed by addition of 2-chloro-*N,N*-dimethylethanamine (92 mg, 0.63 mmol), and the reaction mixture was heated to 60 °C. After 2 h, the reaction mixture was cooled to room temperature, poured in water, and extracted with ethyl acetate. The extract was evaporated to get residue, which was subjected to CC to get compound RTK10.

RESULTS AND DISCUSSION

The dysfunction of lysine acetyltransferases could be associated with several diseases, like asthma, cardiovascular disorders, diabetes, and cancer (10–15). We have established a screening system of medicinal plants (described in the Indian ayurvedic literature, see Ref. 36), for acetyltransferase modulation activity. In this process, we have tested the crude extract of *P. rosea* and eventually isolated plumbagin (RTK1) and crystallized to characterize the compound (Fig. 1*A*, *panel II*).

Plumbagin/RTK1 Inhibits in Vivo Histone Acetylation—RTK1 is a highly cell-permeable compound with important cellular effects like anti-tumor activity (19–22), NF-κB activity,

etc. (23). RTK1 is a potent apoptosis-inducing agent at higher concentrations. Histones (both H3 and H4) are known to be hyperacetylated in hepatocarcinomas (24). To find out the ability of RTK1 to inhibit HAT activity *in vivo*, the liver cancer cell line HepG2 was treated with RTK1 at concentrations that do not induce apoptosis. In agreement with a previous report (24), the histone H3 was found to be substantially acetylated in these cells (Fig. 1*B*, *lane 1*). The acetylated histone H3 level was reduced by 50% with 5 μM RTK1 treatment (Fig. 1*B*, *lane 2*). A dose-dependent inhibition of histone H3 acetylation was observed with almost 90% inhibition on 25 μM RTK1 treatment (Fig. 1*B*, *lane 4*). The overall acetylation status of the histones was also found to be significantly decreased with a prominent reduction of H3 and H4 acetylation (supplemental Fig. 1). Because the HepG2 cells grow in clumps, the immunofluorescence imaging of these cells was difficult. Therefore, the histone acetylation upon plumbagin treatment was verified by immunofluorescence analysis in HeLa cells, wherein the cells were treated with the compound and DMSO (solvent control) for 12 h. Because the acetylation level in HeLa cells is low, histone acetylation was induced by treating with histone deacetylase inhibitors (Fig. 1*C*, *TSA/NaBu*) followed by RTK1 treatment. As expected, RTK1 could inhibit the histone acetylation in HeLa cells efficiently at 5 μM concentration. There was an almost complete reduction in the acetylation levels with 25 μM concentration of RTK1, as visualized by immunofluorescence analysis (Fig. 1*C*, *DMSO versus RTK1*). Furthermore, the HAT inhibition by RTK1 was also confirmed *in vivo* wherein the liver tissue of RTK1-treated mice was examined for inhibition of histone acetylation. As visualized by immunohistochemistry using antibody against acetylated histone H3 (Lys-9 and Lys-14), there was a significant decrease in histone acetylation in RTK1-treated mice liver as compared with the normal and DMSO-treated controls. The acetylation status of histones in the untreated mouse liver was taken as the control for comparing the treated sections (Fig. 1*D*, *panel I*, *H&E staining* and *AcH3 staining*). There was no gross loss in morphology of cells as indicated by the hematoxylin and eosin staining. The solvent control sections show strong to moderate positive staining in hepatocytes near the central vein and portal triad regions indicating the ability of the solvent for inducing the acetylation in these cells (Fig. 1*D*, *panel II*, *H&E staining* and *AcH3 staining*). On the other hand, RTK1 dissolved in the DMSO solvent shows negative staining for Ac-H3 antibody indicating the inhibitory activity of acetylation by RTK1 in this liver sample (Fig. 1*D*, *panel III of H&E staining* and *AcH3 staining*). Taken together, these data suggest that RTK1 inhibits histone acetylation *in vivo*.

Plumbagin/RTK1 Inhibits Non-histone Protein Acetylation by p300—The inhibition of histone acetylation by plumbagin was investigated by an antibody raised against the peptide resembling the histone H3 tail, in which the Lys-9 and Lys-14 residues are acetylated. *In vivo*, these residues are acetylated by HATs p300/CBP and PCAF, which are also referred to as factor acetyltransferases or protein acetyltransferases. This is because of their ability to act on several non-histone substrates leading to distinct functional consequences. p53 is an *in vivo* substrate of both these histone acetyltransferases. p300 and PCAF acetylate different lysine residues (Lys-373 and Lys-320, respectively) of p53 upon DNA damage (25). To investigate any possible specificity of RTK1 to KAT activity in the cellular system, we selected the phenomenon of p53 acetylation. For this purpose, we treated HEK293 cells with different concentrations of RTK1 for 3 h following which acetylation of p53 was enhanced by treating cells with doxorubicin for 6 h. Whole cell lysates prepared from the treated cells (as described above) were subjected to Western blotting analysis using antibodies against p53, acetyl-p53 (Lys-373), acetyl-p53 (Lys-320), and α-tubulin. It was found that the acetylation of p53 at lysine 373 (by p300) was inhibited by treating cells with increasing concentrations of RTK1 (Fig. 2, *panel II, lane 1 versus lanes 2–4*). Significantly, similar concentration of RTK1 did not affect the acetylation of p53 at lysine 320 (by PCAF) (Fig. 2, *panel III, lane 1 versus lanes 2–4*). Levels of p53 and tubulin were used as protein expression controls (Fig. 2, *panels I* and *IV*). Yet another non-histone substrate of p300 is positive cofactor 4 (PC4), whose transcriptional coactivator function on p53 is controlled by its acetylation (26). The *in vitro* acetylation of PC4 by p300 was found to be inhibited by RTK1 in a gel fluorography assay (supplemental Fig. 2). These results establish that indeed RTK1 preferentially targets p300-mediated lysine acetyltransferase activity in the physiological context. Significantly, the treatment of RTK1 in the HepG2 cells did not alter the expression of p300 (data not shown), suggesting that it is the enzymatic activity that is modulated and not the protein expression.

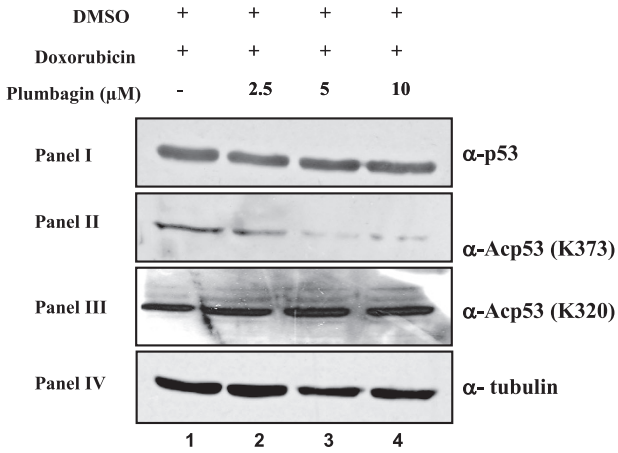

FIGURE 2. **RTK1 inhibits p300-mediated non-histone protein acetylation.** HEK293 cells were treated with either DMSO (*lane 1*) or RTK1 with the indicated concentrations (*lanes 2–4*) for 3 h. Following the treatment, the cells were treated with doxorubicin for 6 h. The cell lysates were subjected to immunoblotting analysis using either anti-acetyl-p53 Lys-373 (*α-Acp53 (K373)*, *panel II*) or anti-acetyl-p53 Lys-320 (*α-Acp53 (K320)*, *panel III*), or anti-p53 DO-1 (*panel I*), or anti-tubulin (*panel IV*). Tubulin and p53 antibody were used to verify the equal amounts of protein loaded into each lane.

Plumbagin/RTK1 Is a p300 HAT Inhibitor—RTK1 could inhibit the histone and non-histone protein acetylation *in vivo* with a specificity toward p300. We further investigated the comparative HAT inhibition activity of RTK1 and other known inhibitors such as anacardic acid, garcinol, isogarcinol, LTK14, and curcumin (Fig. 3*B*). The IC_{50} value of RTK1 with the full-length p300 (supplemental Fig. 3) was found to be similar to that of other p300-specific inhibitors, LTK14 and curcumin

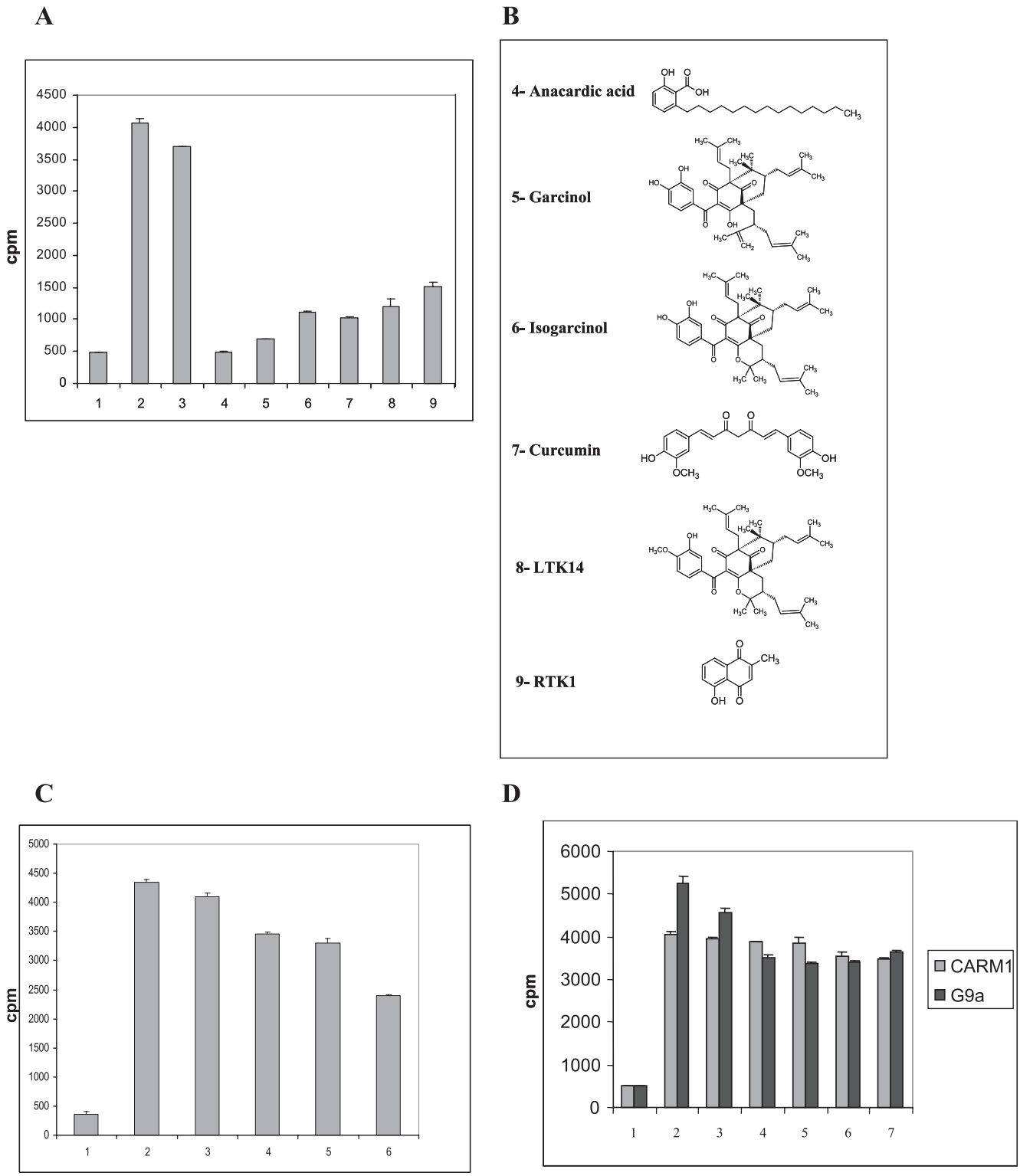

FIGURE 3. **RTK1 is an inhibitor of histone acetyltransferase p300.** *A,* filter binding HAT assay for inhibition of histone acetylation. Assays were performed with hexahistidine-tagged, baculovirus-expressed full-length p300 in the presence or absence of HAT inhibitors at their reported IC_{50} concentrations by using highly purified HeLa core histones. The following core histones are shown: without p300 (*lane 1*); with p300 (*lane 2*); with p300 in the presence of DMSO (*lane 3*); in the presence of anacardic acid (10 μM) (*lane 4*); in the presence of garcinol (10 μM) (*lane 5*); in the presence of isogarcinol (10 μM) (*lane 6*); in the presence of curcumin (25 μM) (*lane 7*); in the presence of LTK14 (20 μM) (*lane 8*); and in the presence of RTK1 (25 μM) (*lane 9*). *Error bars* represent S.D. *B,* chemical structures of the HAT inhibitors are in the following order: anacardic acid (*4*); garcinol (*5*); isogarcinol (*6*); curcumin (*7*); LTK14 (*8*); and RTK1 (*9*). *C,* HAT assay was performed with FLAG-tagged baculovirus-expressed PCAF in the presence or absence of RTK1 by using highly purified human (HeLa) core histones and processed for filter binding assay. Core histones are as follows: without enzyme (*lane 1*); with enzyme (*lane 2*); with enzyme in the presence of DMSO (*lane 3*); with enzyme in the presence of increasing concentration of RTK1, 10, 25, and 50 μM (*lanes 4–6*). *Error bars* represent S.D. *D,* filter binding assay for inhibition of histone (arginine and lysine) methylation. Histone methylation assays were performed either with CARM1 (I) or G9a (II) in the presence or absence of RTK1 by using highly purified HeLa core histones and processed for filter binding assay. Core histones are as follows: without enzyme (*lane 1*); histones with enzyme (*lane 2*); histones with enzyme in the presence of DMSO (*lane 3*); histones with enzyme in the presence of increasing concentrations of RTK1, 10, 25, 50, and 100 μM. *Error bars* represent S.D.

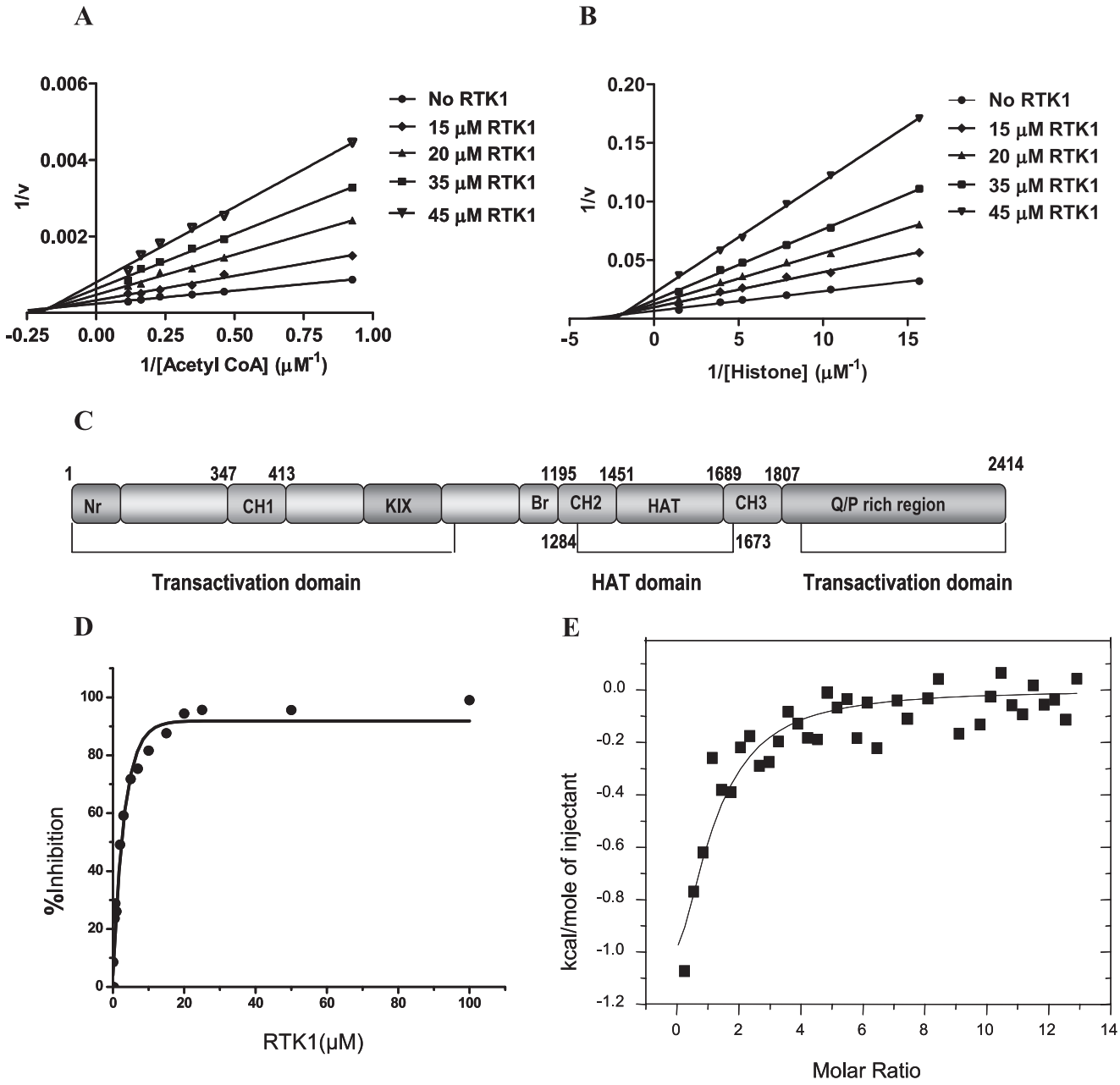

FIGURE 4. **RTK1 is a noncompetitive inhibitor of p300 acetyltransferase activity with a single binding site.** *A* and *B,* kinetics of p300 HAT inhibition by RTK1. *A,* Lineweaver-Burk Plot representation of RTK1-mediated inhibition of p300 HAT activity at a fixed concentration of core histones (1.6 μM) and increasing concentrations of [^{3}H]acetyl-CoA in the presence (15, 20, 35, and 45 μM) or absence of RTK1. *B,* Lineweaver-Burk plot representation of RTK1-mediated inhibition of p300 HAT activity at a fixed concentration of [^{3}H]acetyl-CoA (2.78 μM) and increasing concentrations of core histones in the presence (15, 20, 35, and 45 μM) or absence of RTK1. The results were plotted using the GraphPad Prism software. *C,* domains of histone acetyltransferase p300. Apart from the minimal HAT domain (1284–1673), three CH domains, a single bromodomain, and the KIX domain are present. *D,* percentage of inhibition of HAT activity, performed with p300 minimal HAT domain in the presence or absence of RTK1 (0.5–100 μM), by using highly purified HeLa core histones and processed for filter binding assay. *E,* determination of enthalpy of association of RTK1 with p300 HAT domain. The exothermic heat exchanged per mol of injectant as a function of molar ratio of HAT domain to RTK1. The data were fitted with "one set of sites" binding model. *Solid line* represents the fit of the binding isotherm.

(20–25 μM) (Fig. 3*A*, *lanes 7–9*). However, *in vitro*, it could also inhibit the lysine acetyltransferase PCAF at a higher concentration with an IC_{50} beyond 50 μM (Fig. 3*C*, *lanes, 4–6*). To address the broad spectrum specificity of RTK1 among different chromatin-modifying enzymes, the effect of RTK1 on lysine and arginine methyltransferase activity was also investigated. The results show that even at 100 μM concentration it could not inhibit the methyltransferase activity of G9a (lysine methyltransferase) and CARM1 (arginine methylation) (Fig. 3*D*, *lanes 4–7*). Taken together, these data suggest that RTK1, isolated from a natural source, is an inhibitor of histone acetyltransferases with a preference toward p300.

Plumbagin/RTK1 Is a Noncompetitive Inhibitor of p300 HAT with a Single Binding Site on the Protein—To understand the mechanism of RTK1-mediated inhibition of p300 activity, the enzyme inhibition kinetic analysis was performed. The kinetic analysis of the RTK1-mediated inhibition of p300 acetyltransferase revealed a noncompetitive pattern with both histones

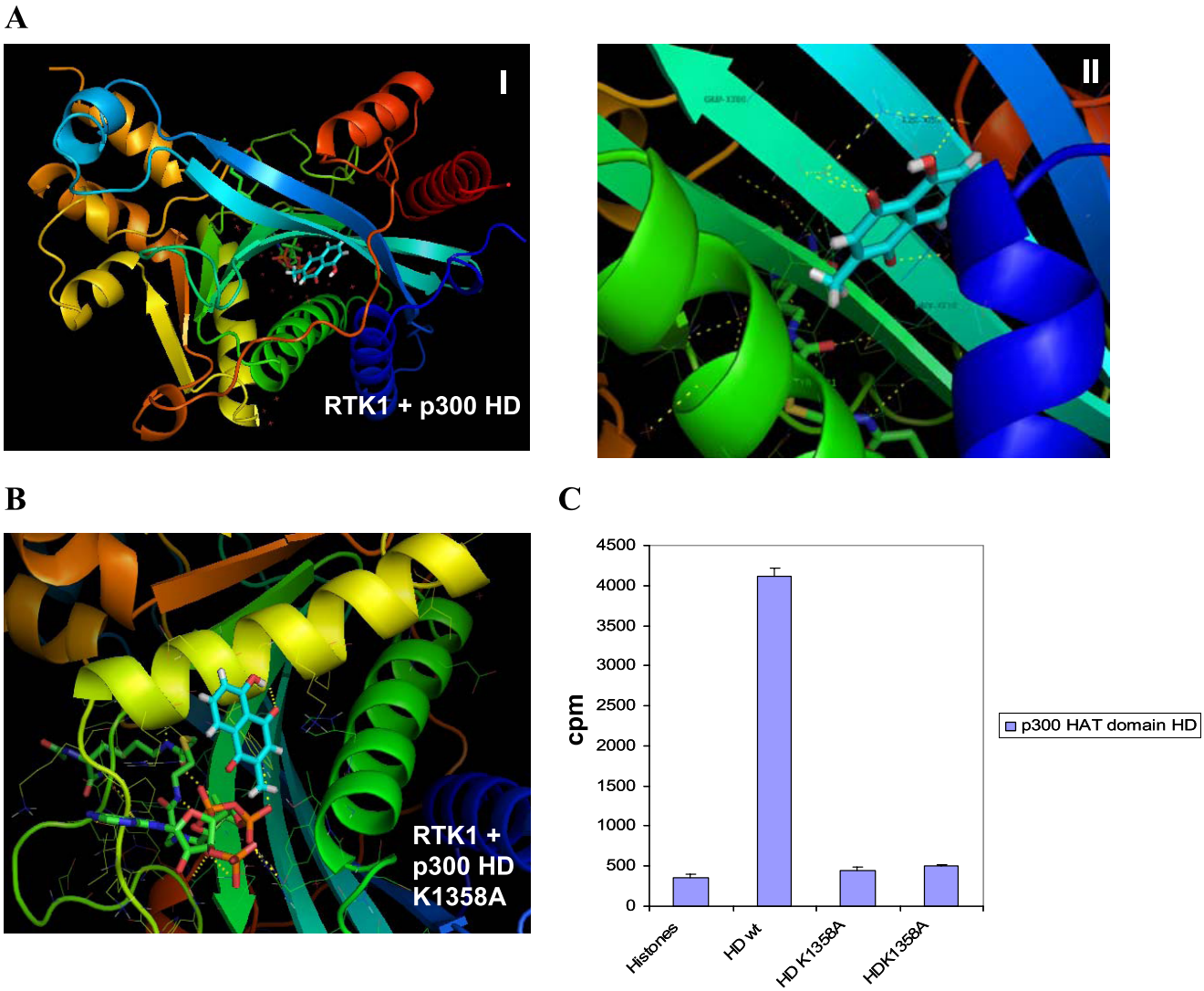

FIGURE 5. **K1358A residue of p300 HAT domain is essential for RTK1 interaction.** *A,* docking of RTK1 onto the p300 HAT domain (*panel I*) and enlarged image of the docking site with the contact residues (*panel II*). *B,* docking of RTK1 onto the *in silico* generated mutant K1358A. *C,* filter binding HAT assay for histone acetylation. Assays were performed with p300 HAT domain (*HD wt* (wild type)) or HAT domain K1358A by using highly purified HeLa core histones. Core histones are shown as follows: without enzyme (*lane 1*); with HAT domain wild type (*lane 2*); with HAT domain K1358A (*lane 3*); and with increased concentration of HAT domain K1358A (*lane 4*). *Error bars* represent S.D.

and acetyl-CoA substrates (Fig. 4, *A* and *B*). The mechanism of inhibition therefore involves the inhibitor binding to a site other than the active site of the enzyme, which was subsequently confirmed by docking studies and also isothermal titration calorimetry.

The baculovirus-expressed full-length p300 often gets degraded and may also contain some interacting proteins even after high quality purification. Because the biophysical experiments require proteins that are highly pure, the subsequent experiments were carried out with the bacterially expressed p300 minimal HAT domain (amino acids 1284–1673). RTK1 inhibits the HAT activity of the p300 catalytically active domain with a very low IC_{50} value of 2 μM indicating the possible interaction of RTK1 with this domain (Fig. 4*D*). RTK1 could inhibit the minimal HAT domain more potently than the full-length p300. There was a reduction in the IC_{50} value (2 μM) for the HAT domain that is 10-fold lower than the IC_{50} value (20 μM) of full-length p300. However, the pattern of HAT inhibition was similar to that of p300 full-length, *i.e.* noncompetitive in nature (supplemental Fig. 4). These results further suggest that RTK1 augments its p300 HAT inhibitory activity by directly targeting the minimal HAT domain of p300, which consists of the region responsible for acetyltransferase activity. Furthermore, it should be noted that full-length p300 has the CH1, CH2, CH3, bromodomain, repressive KIX domain, and the unstructured glutamine-rich region (Fig. 4*C*) (18). The site of interaction of RTK1 may not be easily accessible in the full-length protein because of its multidomain organization. However, in the minimal HAT domain, the interaction site might be easily accessible, which could be the cause of reduction in the IC_{50} value. In agreement with this data, it has been shown that the p300-specific inhibitor LTK14 also has a 10 times lower IC_{50} value with the HAT domain than the full-length enzyme (27).

The binding of the inhibitor to the enzyme was also confirmed from isothermal titration calorimetry studies (Fig. 4*E*).

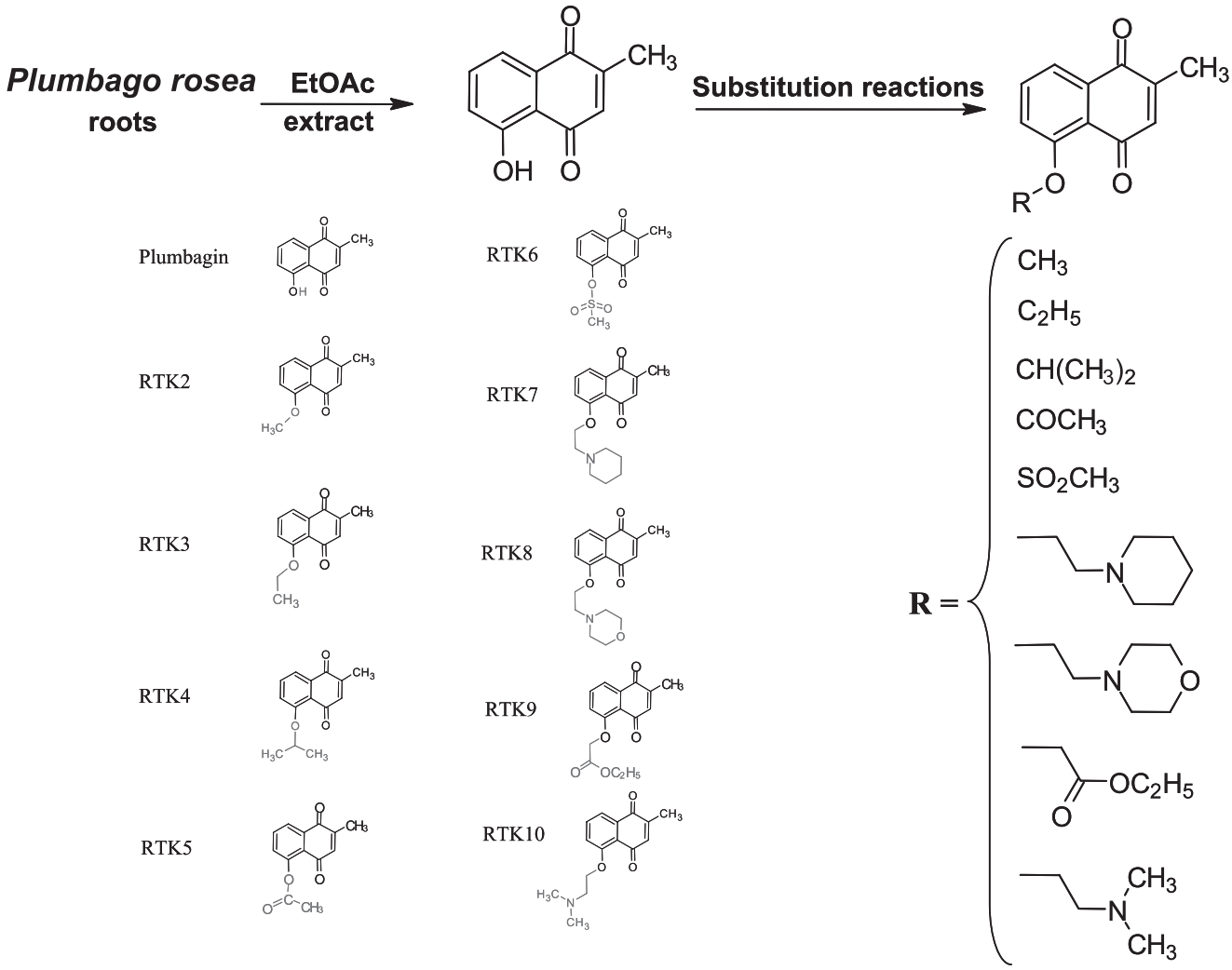

SCHEME 1. **Synthesis scheme and structures of RTK1 and its derivatives (*a–i*).**

The interaction was found to be entropy-driven with high affinity ($K_d = 2 \pm 0.25$ μM, $\Delta H = -2.25 \pm 0.23$ kcal/mol, $\Delta S = 17.2$ entropy units). The binding isotherm could be fitted to a 1:1 stoichiometry. The magnitude of the enthalpy value is consistent with the range of enthalpy values reported for a hydrogen bond such as the one proposed between the RTK1 and p300 HAT domain. The source of positive entropy may be 2-fold as follows: release of bound water from the surface of the protein upon association with the ligand and conformational entropy change of the protein as a sequel to binding. From the above observations, it can be proposed that RTK1 binds to the HAT domain at a single site that is not a part of the active site. The dissociation constant value agrees well with the IC_{50} value (2 μM) as estimated from Fig. 4*D*, thereby supporting the validity of the thermodynamic parameters generated from ITC.

Plumbagin/RTK1 Docks onto the p300 HAT Domain through Hydrogen Bonding to Lys-1358 Residue with Functional Consequences—The crystal structure of the acetyltransferase domain of p300 liganded to a synthetic specific inhibitor, lysyl-CoA (28), has been reported recently. Using this structure, the docking studies with RTK1 have been performed. The p300 HAT domain and inhibitor complex showed an interaction with the hydroxyl group on the 5th carbon in RTK1. The residues involved in the interaction are Lys-1358, Glu-1380, Met-1376, and Tyr-1421 (Fig. 5*A*, *panel I*, and supplemental Fig. 5). As per the docking model, the —OH group interacts with Lys-1358 on the HAT domain and facilitates the further interaction with the remaining three residues (Fig. 5*A*, *panel II*). Because the lysine residue was found to be the primary residue mediating the interaction and the ITC data also suggested a single binding site, this residue (Lys-1358) was mutated to alanine. An *in silico* mutant K1358A was generated that did not show any interaction with the inhibitor (Fig. 5*B*). Subsequently, the same mutant was cloned and expressed. The mutant K1358A showed a similar tryptophan fluorescence spectra as the wild type, suggesting that the overall protein structure was not altered due to the mutation (supplemental Fig. 6, *A* and *B*). Remarkably, this lysine residue was found to be absolutely critical for the HAT activity. It was found that the HAT domain mutant (K1358A) completely lost its acetyltransferase activity in a filter binding assay (Fig. 5*C*). The small molecule inhibitor RTK1 through its hydroxyl group possibly forms a specific interaction with a single lysine residue (Lys-1358) in the p300 HAT domain. The Lys-1358 residue is not a part of the activation loop of p300 and has not been mapped as an important residue in the p300 HAT domain structure. However, one of its adjacent residues, Thr-

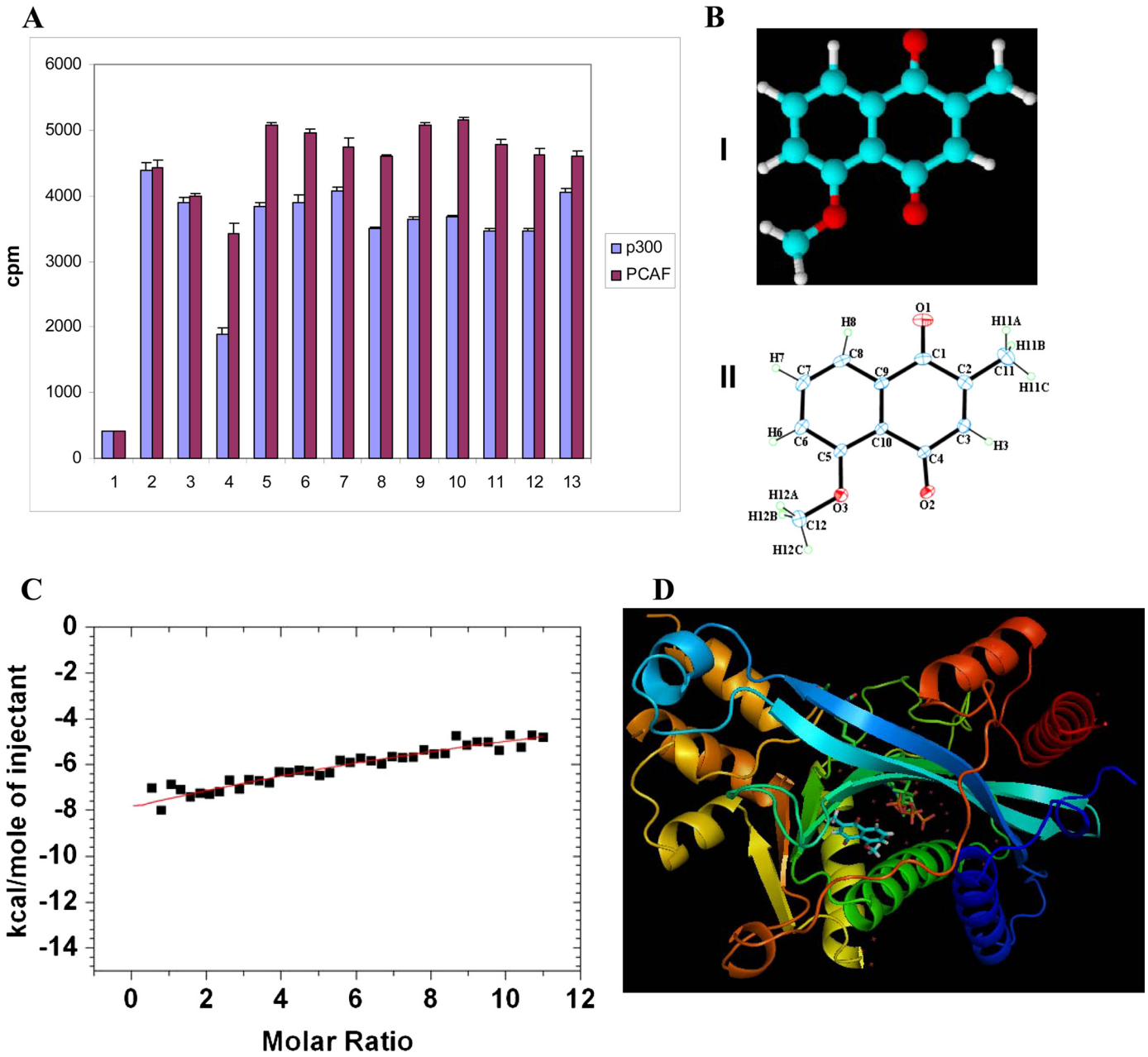

FIGURE 6. **Single hydroxyl group of RTK1 is essential to inhibit p300 HAT activity.** *A,* HAT assays were performed either with p300 (see *I*) or PCAF (see *II*) in the presence or absence of RTK1 and its derivatives by using highly purified HeLa core histones. Core histones are shown as follows: without enzyme (*lane 1*); with enzyme (*lane 2*); with enzyme in the presence of DMSO (*lane 3*); RTK1 (25 μM) (*lane 4*), RTK2-RTK10 (Scheme 1) at 50 μM concentration (*lanes 5–13,* respectively). *Error bars* represent S.D. *B, panel I, ball* and *stick model* of RTK2. where *blue* denotes carbon, *white* indicates hydrogen, and *red* represents oxygen; *panel II,* x-ray crystal structure of RTK2, hydroxyl group substituted by methoxy group. *C,* estimation of enthalpy of association of RTK2 with p300 HAT domain. The exothermic heat exchanged per mol of injectant as a function of molar ratio of HAT domain to RTK2. The data could not be fitted with any binding model giving rational values for enthalpy change and dissociations constant. It implies absence of association. *D,* docking of RTK2 onto the p300 HAT domain.

1357, has been shown to be essential for the structural maintenance of the HAT domain (28). The Thr-1357 residue is a component of the negative environment chamber for the activation loop. Presumably, the Lys-1358 residue also plays an essential role in the activation loop stability directly and/or by affecting the chemical environment around the Thr-1357 residue and hence the acetyltransferase function.

Single Hydroxyl Group of Plumbagin/RTK1 Is Essential for HAT Inhibition—The docking study and the point mutation of K1358A indicated that the single hydroxyl group of RTK1 is possibly involved in interacting with the HAT domain. Therefore, we investigated the chemical entity in "RTK1," which could be involved in the inhibition of p300 HAT activity. RTK1 was derivatized by using the single hydroxyl group at 5th carbon position with various substituents (Scheme 1). Alkyl substitutions at the —OH position, which increased the chain length, could not inhibit HAT activity (Fig. 6*A*, *lanes 5–7*). When groups like acetyl and sulfonyl were substituted for the hydroxyl group of RTK1, a mild reduction (<10%) of HAT activity was observed (Fig. 6*A*, *lanes 8* and *9*). Heterocyclic substitutions such as piperidine, morpholine, and an ester substitution also showed a mild reduction of HAT activity (Fig. 6*A*,

lanes 10–12). However, *N,N*-dimethylamine substituent did not affect the HAT activity (Fig. 6*A*, *lane 13*). As compared with RTK1, all the derivatives were inactive for HAT inhibition at the tested concentration. Thus, the substitution of the hydroxyl group with any other group almost abolishes the inhibition activity, suggesting that the "hydroxyl" group in RTK1 is essential to bring about the HAT inhibition (Fig. 6*A*, *lane 4 versus lanes 5–13*). One of the derivatives, RTK2 (Fig. 6*B*, *panel II*), a methoxy-substituted compound, was crystallized and selected as a representative of the inactive molecules for the detailed characterization. An ITC study with the RTK2 and p300 HAT domain was carried out. The enthalpy change corresponding to the addition of the RTK2 to the p300 HAT domain could not be fitted to any binding model as apparent from the improbable large values of standard errors of deviation (binding site n = 1.06 ± 338, ΔH = 946 ± 30,000 kcal/mol). It implies the absence of any physical association of the —OH group substituted derivative, RTK2, with the p300 HAT domain (Fig. 6*C*). This is in contrast with the strong interaction of RTK1 with the p300 HAT domain. It was further supported from the docking analysis of the HAT domain with RTK2, which does not show the formation of a hydrogen bond or any other interaction with RTK2 (Fig. 6*D*). These data argue for the mechanistic and structural requirements of the —OH group to facilitate the p300 HAT inhibition.

We have earlier shown that several natural compounds, like anacardic acid, curcumin, garcinol possess HAT inhibitory activity. Interestingly, all these molecules are hydroxyl compounds (Fig. 3*B*). The recently reported acetyltransferase inhibitor from a natural source, epigallocatechin 3-gallate, is also a polyhydroxy compound (29). Anacardic acid has a single hydroxyl group and is a potent and nonspecific inhibitor of HATs. The amide derivative of anacardic acid, *N*-(4-chloro-3-trifluoromethylphenyl)-2-ethoxybenzamide), instead of being an inhibitor had HAT activation properties (30). A detailed derivatization study of these amides revealed the importance of the pentadecyl hydrocarbon chain and the presence of electronegative groups ($-CF_3$, $-Cl$) at the para position for the HAT activation (31). Curcumin, a natural p300-specific inhibitor (32), also has two hydroxyl groups. Garcinol, a polyhydroxyl benzophenone, which has three hydroxyl groups, is a potent nonspecific HAT inhibitor (16) with high cellular permeability and cellular toxicity. The cyclization of garcinol, through the enolic hydroxyl group, yielded isogarcinol. Although isogarcinol retained the nonspecific HAT inhibitory activity, it was found to be less potent (with higher IC_{50}) as compared with garcinol. The 14-monomethyl-substituted derivative of isogarcinol, LTK14, has a single hydroxyl group (17). This derivative is a specific inhibitor of p300 and is almost nontoxic in nature. However, LTK14 is a less potent inhibitor in comparison with garcinol. This raises the possibility that multiple hydroxyl groups in garcinol might be responsible for its potent HAT inhibition ability. In agreement with our present finding, the disubstitution of isogarcinol yielded compounds (devoid of any hydroxyl groups) that could not inhibit the HAT activity. The only exception is the methylsulfonyl-disubstituted isogarcinol (LTK19), which was also found to be a p300-specific inhibitor (17). However, the similar functional group substitution in RTK1 did not show any inhibitory activity (Fig. 6*A*, *lane 9*).

In summary, we have identified a small molecule inhibitor of the KAT, p300, from a natural source, which offered the opportunity to identify the chemical entity responsible for the inhibition of the KAT activity. All the natural KAT inhibitors (specific and nonspecific) discovered so far possess a hydroxyl group. We have shown that substitution of a single hydroxyl group with any functional group (see Scheme I) present in plumbagin/RTK1 completely ceases its ability to inhibit the KAT activity. These data suggest that possibly the hydroxyl group-mediated interaction of RTK1 with p300 could be essential for the inhibition of acetyltransferase activity, as hypothesized previously (33). This presumption could be general and might be one of the mechanisms associated with HAT inhibition by these inhibitors. Interestingly, in the p300 minimal HAT domain, a novel site, Lys-1358, has been identified that is essential for the acetyltransferase activity of p300. This residue is not a part of the catalytic site nor the activation loop as suggested earlier (28), yet it regulates the enzyme function. The exact role of this residue needs to be characterized. Furthermore, the interaction of the other p300 HAT inhibitors with this critical residue also needs to be investigated. Plumbagin has been reported to suppress NF-κB activation leading to the potentiation of apoptosis (23). Because the process of NF-κB activation requires p300-mediated acetylation of the p65 subunit of NF-κB, the suppression observed could be due to the p300-specific inhibition in the physiological condition. Although plumbagin is a putative anticancer agent (19–22), its major limitation for use as therapeutic molecule could be the cellular toxicity. Synthesis of efficient nontoxic p300-specific KAT inhibitors, with an intact hydroxyl group, could be highly useful both as a therapeutic as well as a biological tool for modulating acetyltransferase function. However, we hope that these data could be highly useful in designing therapeutically favorable novel acetyltransferase inhibitors from the natural compound.

Acknowledgments—We thank B. S. Suma for confocal microscopy (Molecular Biology and Genetics Unit), G. Nagashankar for assistance with immunohistochemistry (x-ray crystallography facility of Chemistry and Physics of Materials Unit, Jawaharlal Nehru Centre for Advanced Scientific Research), and Dr. Kiran Batta for PC4 protein.

REFERENCES

1. Batta, K., Das, C., Gadad, S., Shandilya, J., and Kundu, T. K. (2007) *Chromatin and Disease,* Vol. 41, pp. 193–212 Springer Publications, London
2. Roth, S. Y., Denu, J. M., and Allis, C. D. (2001) *Annu. Rev. Biochem.* **70,** 81–120
3. Swaminathan, V., Reddy, B. A., Ruthrotha Selvi, B., Sukanya, M. S., and Kundu, T. K. (2007) *Chromatin and Disease,* Vol. 41, pp. 397–428 Springer Publications, London
4. Grant, P. A., and Berger, S. L. (1999) *Semin. Cell Dev. Biol.* **10,** 169–177
5. Giles, R. H., Peters, D. J., and Breuning, M. H. (1998) *Trends Genet.* **14,** 178–183
6. Giordano, A., and Avantaggiati, M. L. (1999) *J. Cell. Physiol.* **181,** 218–230
7. Goodman, R. H., and Smolik, S. (2000) *Genes Dev.* **14,** 1553–1577
8. Chan, H. M., and La Thangue, N. B. (2001) *J. Cell Sci.* **114,** 2363–2373
9. Heery, D. M., and Fischer, P. M. (2007) *Drug Discov. Today* **12,** 88–99
10. Zheng, Y., Thompson, P. R., Cebrat, M., Wang, L., Devlin, M. K., Alani,

R. M., and Cole, P. A. (2004) *Methods Enzymol.* **376,** 188–199
11. Stimson, L., Rowlands, M. G., Newbatt, Y. M., Smith, N. F., Raynaud, F. I., Rogers, P., Bavetsias, V., Gorsuch, S., Jarman, M., Bannister, A., Kouzarides, T., McDonald, E., Workman, P., and Aherne, G. W. (2005) *Mol. Cancer Ther.* **4,** 1521–1532
12. Iyer, N. G., Chin, S. F., Ozdag, H., Daigo, Y., Hu, D. E., Cariati, M., Brindle, K., Aparicio, S., and Caldas, C. (2004) *Proc. Natl. Acad. Sci. U.S.A.* **101,** 7386–7391
13. Davidson, S. M., Townsend, P. A., Carroll, C., Yurek-George, A., Balasubramanyam, K., Kundu, T. K., Stephanou, A., Packham, G., Ganesan, A., and Latchman, D. S. (2005) *ChemBioChem* **6,** 162–170
14. Zhou, X. Y., Shibusawa, N., Naik, K., Porras, D., Temple, K., Ou, H., Kaihara, K., Roe, M. W., Brady, M. J., and Wondisford, F. E. (2004) *Nat. Med.* **10,** 633–637
15. Varier, R. A., and Kundu, T. K. (2006) *Curr. Pharm. Des.* **12,** 1975–1993
16. Balasubramanyam, K., Altaf, M., Varier, R. A., Swaminathan, V., Ravindran, A., Sadhale, P. P., and Kundu, T. K. (2004) *J. Biol. Chem.* **279,** 33716–33726
17. Mantelingu, K., Reddy, B. A., Swaminathan, V., Kishore, A. H., Siddappa, N. B., Kumar, G. V., Nagashankar, G., Natesh, N., Roy, S., Sadhale, P. P., Ranga, U., Narayana, C., and Kundu, T. K. (2007) *Chem. Biol.* **14,** 645–657
18. Arif, M., Kumar, G. V., Narayana, C., and Kundu, T. K. (2007) *J. Phys. Chem. B* **111,** 11877–11879
19. Kuo, P. L., Hsu, Y. L., and Cho, C. Y. (2006) *Mol. Cancer Ther.* **5,** 3209–3221
20. Hsu, Y. L., Cho, C. Y., Kuo, P. L., Huang, Y. T., and Lin, C. C. (2006) *J. Pharmacol. Exp. Ther.* **318,** 484–494
21. Gomathinayagam, R., Sowmyalakshmi, S., Mardhatillah, F., Kumar, R., Akbarsha, M. A., and Damodaran, C. (2008) *Anticancer Res.* **28,** 785–792
22. Acharya, B. R., Bhattacharyya, B., and Chakrabarti, G. (2008) *Biochemistry* **47,** 7838–7845
23. Sandur, S. K., Ichikawa, H., Sethi, G., Ahn, K. S., and Aggarwal, B. B. (2006) *J. Biol. Chem.* **281,** 17023–17033
24. Bai, X., Wu, L., Liang, T., Liu, Z., Li, J., Li, D., Xie, H., Yin, S., Yu, J., Lin, Q., Zheng, S. (2008) *J. Cancer Res. Clin. Oncol.* **134,** 83–91
25. Sakaguchi, K., Herrera, J. E., Saito, S., Miki, T., Bustin, M., Vassilev, A., Anderson, C. W., and Appella, E. (1998) *Genes Dev.* **12,** 2831–2841
26. Batta, K., and Kundu, T. K. (2007) *Mol. Cell. Biol.* **27,** 7603–7614
27. Arif, M., Pradhan, S. K., Thanuja, G. R., Vedamurthy, B. M., Agrawal., S., Dasgupta, D., and Kundu, T. K. (2009) *J. Med. Chem.* **52,** 267–277
28. Liu, X., Wang, L., Zhao K., Thompson, P. R., Hwang, Y., Marmorstein, R., and Cole, P. A. (2008) *Nature* **451,** 846–850
29. Choi, K. C., Jung, M. G., Lee, Y. H., Yoon, J. C., Kwon, S. H., Kang, H. B., Kim, M. J., Cha, J. H., Kim, Y. J., Jun, W. J., Lee, J. M., and Yoon, H. G. (2009) *Cancer Res.* **69,** 583–592
30. Balasubramanyam, K., Swaminathan, V., Ranganathan, A., and Kundu, T. K. (2003) *J. Biol. Chem.* **278,** 19134–19140
31. Mantelingu, K., Kishore, A. H., Balasubramanyam, K., Kumar, G. V., Altaf, M., Swamy, S. N., Selvi, R., Das, C., Narayana, C., Rangappa, K. S., and Kundu T. K. (2007) *J. Phys. Chem. B* **111,** 4527–4534
32. Balasubramanyam, K., Varier, R. A., Altaf, M., Swaminathan, V., Siddappa, N. B., Ranga, U., and Kundu, T. K (2004) *J. Biol. Chem.* **279,** 51163–51171
33. Sarli, V., and Giannis, A. (2007) *Chem. Biol.* **14,** 605–606
34. Lau, O. D., Kundu, T. K., Soccio, R. E., Ait-Si-Ali, S., Khalil, E. M., Vassilev, A., Wolffe, A. P., Nakatani, Y., Roeder, R. G., and Cole, P. A. (2000) *Mol. Cell* **5,** 589–595
35. Biel, M., Kretsovali, A., Karatzali, E., Papamatheakis, J., and Giannis, A. (2004) *Angew. Chem. Int. Ed. Engl.* **43,** 3974–3976
36. Dinda, B., Das, S. K., and Hajra, A. K. (1995) *Indian J. Chem.* **34B,** 525–528